ELSEVIER

Cardiovascular Pathology 20 (2011) 343 – 351

CARDIOVASCULAR PATHOLOGY

Original Article

Mechanical function, glycolysis, and ultrastructure of perfused working mouse hearts following thoracic aortic constriction

Michael E. Dunn[a], Thomas G. Manfredi[b], Arthur C. Cosmas[b], Frederick J. Vetter[c], Joshua N. King[b], Robert L. Rodgers[a,*]

[a]*Department of Biomedical and Pharmaceutical Sciences, University of Rhode Island, Kingston, RI 02881, USA*
[b]*Department of Kinesiology, University of Rhode Island, Kingston, RI 02881, USA*
[c]*Department of Electrical, Computer and Biomedical Engineering, University of Rhode Island, Kingston, RI 02881, USA*

Received 15 September 2010; received in revised form 2 November 2010; accepted 13 December 2010

Abstract

Background: Glycolytic flux in the mouse heart during the progression of left ventricular hypertrophy (LVH) and mechanical dysfunction has not been described. **Methods:** The main objectives of this study were to characterize the effects of thoracic aortic banding, of 3- and 6-week duration, on: (1) left ventricular (LV) systolic and diastolic function of perfused working hearts quantified by analysis of pressure–volume loops; (2) glycolytic flux in working hearts expressed as the rate of conversion of ^{3}H-glucose to ^3H_2O, and (3) ultrastructure of LV biopsies assessed by quantitative and qualitative analysis of light and electron micrographs. **Results:** Results revealed that (1) indexes of systolic function, including LV end-systolic pressure, cardiac output, and rate of LV pressure development and decline, were depressed to similar degrees at 3 and 6 weeks post-banding; (2) diastolic dysfunction, represented by elevated LV end-diastolic pressure and volume, was more severe at 6 than at 3 weeks, consistent with a transition to failure; (3) a progressive decline in glycolytic flux that was roughly half the control rate by 6 weeks post-banding; and (4) structural derangements, manifested by increases in interstitial collagen content and myocyte Z-band disruption, that were more marked at 3 weeks than at 6 weeks. **Conclusion:** The results are consistent with the view that myocyte damage, fibrosis, and suppressed glycolytic flux represent maladaptive structural and metabolic remodeling that contribute to the development of failure in high pressure load-induced LVH in the mouse. Published by Elsevier Inc.

Keywords: Working perfused heart; Mouse; Cardiac hypertrophy; Metabolism

1. Introduction

Aortic banding or constriction (transverse, thoracic, or abdominal) is a common experimental approach to inducing pathological left ventricular hypertrophy (LVH). In general, the resulting high pressure loads over time produce hypertrophic heart failure (HF) characterized by elevations in ventricular diastolic pressures and volumes in vivo [1-3] and fibrotic changes manifested primarily by increases in ventricular collagen deposition [4,5]. The prevailing view is that LVH of various etiologies is also associated with increases in the utilization of glucose, particularly the rate of glycolysis [6,7] and that this effect represents adaptive metabolic remodeling in chronic HF [8,9].

The mouse model is being used increasingly to assess cardiac function under normal and pathological conditions both in vivo [1,10] and ex vivo [11,12], primarily because the mouse is uniquely subject to genetic manipulation [13]. Advantages of the perfused working heart technique, compared to the analysis of cardiac function in vivo, include the ability to rigidly define and control external loading conditions and perfusate content and to reliably generate myocardial functional and metabolic profiles simultaneously in one preparation. Nevertheless, most or all of the available information regarding effects of high pressure loads on mouse heart function has been obtained in vivo [1,14], where loading conditions and neurohormonal influences are not

* Corresponding author. Department of Biomedical and Pharmaceutical Sciences University of Rhode Island, Kingston, RI 02881, USA. Tel.: +1 401 874 5033; fax: +1 401 874 7949.
E-mail address: rrodgers@uri.edu (R.L. Rodgers).

1054-8807/10/$ – see front matter. Published by Elsevier Inc.
doi:10.1016/j.carpath.2010.12.003

rigidly controlled, and in which assessment of myocardial fuel utilization is much more problematic.

To our knowledge, there are no studies of the effects of aortic banding in the mouse on either mechanical function assessed ex vivo or on glycolytic flux in any preparation. In addition, simultaneous changes in functional, metabolic, and ultrastructural characteristics, in any experimental model of chronic hypertrophic HF, have apparently not been described in a single report. Such a study would help to clarify the respective contributions of functional, metabolic, and structural remodeling to the development of heart failure in high pressure load-induced LVH. Accordingly, the focus of this report was to characterize left ventricular (LV) performance, glycolytic flux, and ventricular ultrastructure of perfused working hearts isolated from mice 3 and 6 weeks after thoracic aortic banding.

2. Methods

2.1. Experimental animals and aortic banding procedure

Male C57BL/6 mice were housed in temperature-controlled quarters (21°C) with a 12-h light/dark cycle. Thoracic aortic banded (TAB) and non-banded controls were purchased from Taconic Farms (New York, NY, USA). Surgical procedures were performed by the vendor on 8–10-week-old animals. Briefly, a 23G blunted needle was passed under the thoracic aortic arch of buprenorphine-anesthetized mice, tied with 5-0 silk, and then removed leaving the aorta partially constricted. Sham-operated mice were treated identically except that the aortas were not ligated. Animals were allowed to recover and shipped seven days post surgery. Preliminary studies indicated that heart performance, metabolism, and cardiomyocyte structure of sham-operated mice and intact C57BL/6 mice—that had not undergone the surgical procedure—were not different. Therefore, the nonbanded groups consist of pooled data from sham-operated and intact animals. Successful banding was verified by consistent increases in heart weights (Table 1).

2.2. Perfused working mouse heart procedure

The method of mouse heart perfusion is similar to the working rat heart preparation [15,16] but modified to accommodate the reduced heart size. Mice were administered an intraperitoneal injection of heparin (40 U) 15 min prior to rapid cervical dislocation. The heart was excised and arrested in cold Krebs-Henseleit (KH) solution containing (in mM) NaCl, 120; $CaCl_2 \cdot {}^2H_20$, 1.8; $NaHCO_3$, 25; $NaH_2PO_4 \cdot H_20$, 1.2; $MgS0_4 \cdot {}_7H_20$ 0.65; KCl, 5.6; and glucose, 11 and then rapidly trimmed of lungs and additional tissue. The aorta was cut just proximal to the carotid branch and temporarily affixed to a 21G blunted needle using a 1.5 mm micro-vascular clip. The aortic remnant was then permanently secured to the cannula using 5-0 silk. The coronary arteries were first perfused via the aorta in the Langendorff mode with KH solution (pH 7.4) gassed with 95% O_2/5% CO_2 at 37°C. Aortic pressure was set at 100 cm H_2O [17]. During retrograde perfusion, the left atrium was cannulated with a 2-mm, 18G blunted needle. The hearts were then switched to the working mode, with left atrial filling pressure set at 10 cM H_2O. Resistance to aortic outflow was 16.4 mm Hg ml^{-1} min^{-1}, generated by a 19 cm length of PE-30 tubing connected to the aortic outflow. Following 10 min of stabilization, mechanical function of spontaneously beating hearts was assessed over 1–2 min. The hearts were then paced at 315 beats per minute, unless the spontaneous rate was higher, and the rate of glycolysis was then determined in a subset of hearts in each group for 40 min. The perfusate was 55 ml of KH buffer solution additionally containing 0.4 mM palmitate, 11 mM glucose, and 3% bovine serum albumin (Sigma-Aldrich, St. Louis, MO, USA) dialyzed overnight using a Spectra/Por 1 membrane with a MW cutoff of 6–8 kDa (Spectrum, Rancho Dominguez, CA, USA), and gassed with 95% O_2/5% CO_2 (pH 7.4).

2.3. Analysis of myocardial function

Left ventricular pressure and volume measurements were obtained using a 1.4F Mikro-Tip (Millar Instruments, Houston, TX, USA) catheter inserted directly into the LV chamber through a hole created by puncturing the apex with a 27G needle. The average of five successive beats was used for functional and statistical analysis at each sample time. External pressure calibration of the catheter was performed using a mercury filled manometer. Volume calibration was determined using both an external plastic chamber and a potassium-arrested mouse heart. The

Table 1
Body and organ measurements

	HW (mg)	BW (g)	HW/BW (mg/g)	HW/FW (mg/g)	LW (mg)	LW/BW (mg/g)
3-wk Control (n=8)	168±8	26.5±0.8	6.4±0.3	4.1±0.2	166±8	6.2±0.2
3-wk TAB (n=18)	211±12 *	25.2±0.4	8.3±0.5	5.3±0.3 *	167±7	6.6±0.3
6-wk Control (n=9)	187±6	28.5±0.8	6.5±0.5	4.3±0.2	157±5	5.5±0.2
6-wk TAB (n=8)	268±27 *	25.4±1.0 *	10.9±1.5 *	6.8±0.8 *	229±46 *	9.5±2.3 *

Body, organ, and bone weights of TAB and age-matched non-banded mice at 3 and 6 weeks post banding. Values are means±S.E.M.
HW, heart weight; BW, body weight; FW, femur weight; LW, lung weight.
* Significantly different from age-matched non-banded group, $P<.05$.

correction factor [(catheter reading−20)/0.5] was obtained by linear regression of the pooled known vs. readout volume values (r^2=0.98). The catheter was linked to a Millar MPVS-300 Pressure-Volume Control Unit and integrated into a Data Acquisition Omni CD program (Data Translation, Marlboro, MA, USA). Analysis of cardiac function data was performed using the Millar PVAN Data Analysis software (Millar Instruments). Coronary flow rates are reported as the difference between aortic flow (measured volumetrically) and cardiac output (from pressure–volume loops).

2.4. Measurement of glycolytic flux

Glycolysis was quantified as the rate of conversion of 5-^{3}H glucose to ^3H_2O. After analysis of ventricular function, 20 μl D-[5-^{3}H(N)]-glucose (PerkinElmer, Boston, MA, USA) was added to the perfusate (average specific activity≈59,000 cpm/μmol). After an additional 20 min, 200-μl perfusate samples were obtained every 5 min for 40 min. The rate of myocardial glycolysis was determined as previously described for rat hearts [18] with minor modifications for the mouse. Briefly, perfusate samples (180 μl) were passed over borate-treated Dowex 1×4–400 ion exchange resin (Sigma-Aldrich) columns in 14cm Pasteur pipettes. Preliminary studies verified 100% separation of ^3H_2O from ^{14}C-glucose, with 95% yield of ^3H_2O, using this procedure. The amount of tritiated water was quantified using a Beckman LS 5000TD scintillator. The rate of glycolytic flux was calculated from the specific activity and dry heart weights (directly determined for each heart) and expressed as the slope of the regression line over 40 min. Values were expressed as micromoles of glucose per minute per gram of dry weight. Dry-to-wet heart weight ratios (mg/g) of the TAB hearts were somewhat lower than those of the non-banded group: 155±4 and 180±3, respectively (P<.05). Peak LV pressure remained stable during the 40-min sampling period in both the TAB and non-banded control groups. All animal care protocols and experimental procedures were approved by the University of Rhode Island Institutional Animal Care and Use Committee in accordance with state and federal guidelines.

2.5. Tissue collection

Tissue samples were collected at 3 and 6 weeks post surgery (n=20) from nonperfused hearts following rapid cervical dislocation. Left ventricular apex biopsies (1-mm cubes) were immediately placed in paraformaldehyde and 1.4% gluteraldehyde in buffered 0.1 M sodium cacodylate fixative at 4°C. Tissue was fixed for a minimum of 72 h then post-fixed in osmium tetroxide in sodium cacodylate buffer for 48 h. Following buffer rinses and dehydration treatment in ethanol and propylene oxide, the tissue samples were flat embedded in Epon 812 and placed in a 70°C oven to polymerize for 48 h.

2.6. Microscopic analysis

Ultrathin cross and longitudinal sections were cut using a diamond knife and a Dupont Sorval MT2B ultramicrotome. Sections were collected on pre-cleaned 200 mesh copper grids and stained with uranyl acetate and lead citrate for 2–7 min each. Upon completion of the staining, grids were gently washed with deionized water, blotted with filter paper and allowed to dry. Stained grids were analyzed using a Philips 301 transmission electron microscope.

Images were quantitatively analyzed at 5700× using a 1024×768 capture resolution setting with a Lumenera Scientific Infinity 2 side-column mounted digital camera linked to a desktop computer and analyzed using National Institutes of Health (NIH) Image J. A stereological point counting procedure (192-point cross grid) was used to quantify the damaged Z-band fraction (DZF), expressed per unit fiber area [19]. Damaged Z-bands were defined as any Z-band that exhibited non-linear characteristics including streaming and dissolution. Values for individual grids were obtained by counting the number of cross grids that intersected with the structure of interest and expressed as a percentage of total grid points. Reported group mean values (±S.E.M.) were calculated from individual averages of ten analyzed images per tissue sample [19]. Images were also qualitatively analyzed at magnifications ranging from 4500–45,000×.

Left ventricular apex collagen content was analyzed using an Olympus BX51 light microscope equipped with an Olympus DP-11 camera; 1–5-μm sections were triple-stained using methylene blue, azure II, and basic fuschin. Threshold analysis was performed on stained tissue samples using NIH Image J. Left ventricular collagen content was calculated as the fraction of the nonvascular area occupied by collagen, not including the endocardial and epicardial surfaces [20].

2.7. Statistics

Statistical significance of within-group means were assessed by the unpaired Student's t test, and significance of between-group means was analyzed by one-way analysis of variance followed up with a Games-Howell post hoc test. A calculated P value of < 0.05 was considered significant; lower values were not reported.

3. Results

3.1. Body, organ, and bone weights

TAB produced declines in body weight (BW) and increases in heart weight (HW) and lung weight (LW) at 3 and 6 weeks post banding (Table 1). Ratios of HW/BW and LW/BW were significantly elevated in TAB mice at both 3 and 6 weeks. In addition, LW and LW/BW ratios of TAB

mice were normal at 3 weeks but elevated at 6 weeks post-banding. These changes in heart and lung weights were indicative of marked LVH progressing to HF.

3.2. Cardiac function

Aortic banding produced impairments in both systolic and diastolic function, but the temporal patterns were somewhat different. Marked declines in LV systolic function were equally severe at 3 and 6 weeks post-banding (Table 2 and Fig. 1). Several indices of LV systolic function were depressed, including end-systolic pressure, cardiac output (CO), stroke volume (SV) and LV +dP/dt (Table 2). The decline in stroke work was most pronounced at 3 weeks, followed by a relative improvement 6 weeks following banding, indicative of a compensatory response to the induced pressure overload. In contrast, diastolic dysfunction tended to intensify with duration of banding. This was typified most prominently by the progressive increases in LV end-diastolic pressure (LVEDP) (Fig. 2), LV end-diastolic volume (LVEDV), and possibly LV end-systolic pressure (LVESP) over time (Table 2). These changes were evident from the narrowing and rightward shifts of the LV P-V loops (Fig. 3). Thus, aortic banding produced a rapidly developed and sustained deficit of systolic LV function but a progressive deterioration of diastolic function, confirming the delayed onset of HF in this model.

3.3. Glycolytic flux

The rate of glycolysis was also markedly affected by aortic banding (Fig. 4). In the non-banded mouse hearts, glycolysis appeared to decline somewhat over 6 weeks, but the rates at 0 and 6 weeks were not statistically different. In contrast, glycolysis of the TAB mouse hearts declined steadily over the same time, so that by 6 weeks it was significantly lower (by approximately 45%) than that of the age-matched controls. Regression analysis showed that the slopes of the TAB and control groups were significantly different: controls, −0.09±0.13 (ns); TAB, −0.41±0.09 ($P<.05$). Thus, glycolysis declined steadily and significantly over time in the TAB hearts, roughly paralleling the progressive deterioration of diastolic LV function and onset of HF.

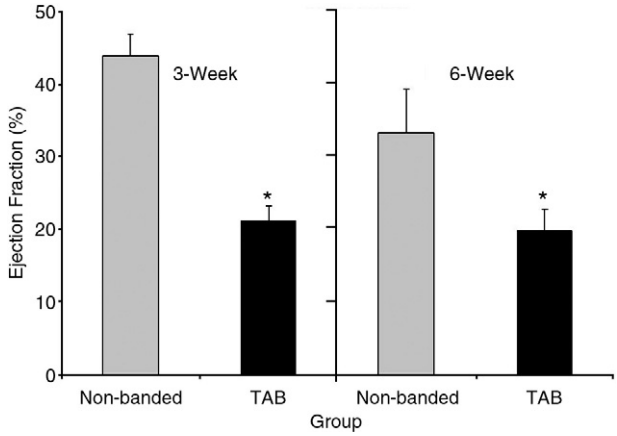

Fig. 1. Ejection fraction. Values are means±S.E.M. *Significantly different from age-matched non-banded group, $P<.05$.

3.4. Myocardial ultrastructure

Structural abnormalities were associated with the establishment of LVH in TAB hearts (Fig. 5). At 3 weeks, the most prominent derangement was a pronounced and significant increase in the DZF compared to the non-banded group (Figs. 5 and 6). Significantly, the extent of damage to Z-bands was much more pronounced at 3 weeks than it was at 6 weeks post-banding. Qualititative observations were consistent with the quantitative results. They revealed no

Table 2
Left Ventricular function in working mouse hearts

	3 Weeks		6 Weeks	
	Sham	TAB	Sham	TAB
Heart rate (bpm)	317±12	283±13	305±15	278±25
End-systolic volume (μl)	63±4	88±5 *	63±8	103±10 *,#
End-diastolic volume (μl)	91±5	104±6	87±7	121±7 *,#
End-systolic pressure (mmHg)	93±5	54±5 *	90±5	61±11 *
Stroke volume (μl)	40±2	22±2 *	29±4 #	24±3 *
Cardiac output (μl/min)	12757±1058	6356±643 *	8695±1302	6871±1277 *
Aortic flow (μl/min)	2720±177	1650±85 *	3100±130	1883±1302 *
Coronary flow rate (ml/min per gram wet heart weight)	58.89±5.64	25.39±4.45 *	31.53±7.19	25.15±6.51
Stroke work (mmHg*μl)	2125±593	433±71 *	1418±174	1284±374
dP/dt max (mmHg/s)	5012±340	2991±194 *	4720±587	3174±473 *
dP/dt min (mmHg/s)	−3453±288	−2197±184 *	−3499±426	−2442±393 *

Measurements of LV function in perfused working hearts from TAB and age-matched non-banded mice at 3 and 6 weeks post-banding. Values are means±S.E.M.
* Significantly different from age-matched non-banded group $P<.05$.
# Significantly different from 3 week banded group, $P<.05$.

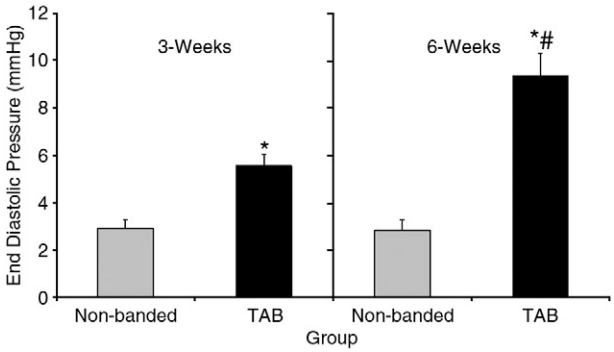

Fig. 2. End diastolic pressure. Values are means± S.E.M. *Significantly different from age-matched non-banded group, $P<.05$; #significantly different from 3-week banded group, $P<.05$.

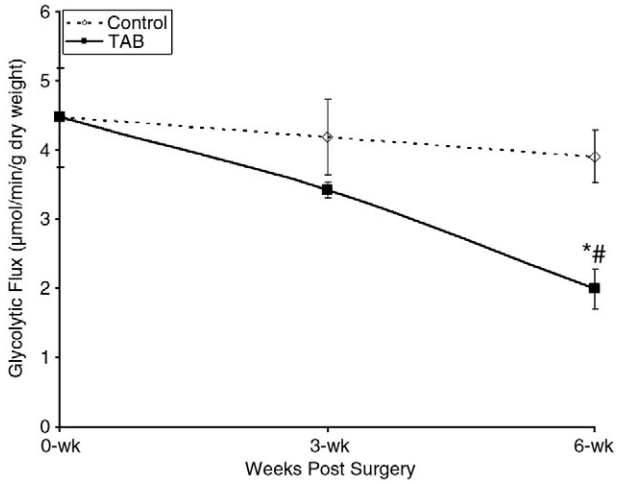

Fig. 4. Glycolytic flux in working perfused hearts from TAB and age-matched non-banded mice at 3 and 6 weeks post-banding. Values are means± S.E.M. *Significantly different from age-matched non-banded group, $P<.05$; #significantly different from 3-week banded group, $P<.05$.

observable alterations in mitochondrial structural integrity of TAB mouse cardiomyocytes but did indicate extensive extramitochondrial damage. The latter consisted of disorganized myofibrils, disruption of sarcomeric organization, swollen sarcotubular elements, increases in intermyofibrillar subsarcolemmal spacing, a loss of myofilaments and organelles in the sarcolemmal area, and an increased number of lysosomes. None of these abnormalities was evident in the age-matched, non-banded controls. Deposition of collagen adjacent to cell borders in the TAB LV tissue was evident at 3 weeks post-banding (Fig. 7). At 6 weeks post-banding, collagen deposition was still evident but was relatively less extensive and appeared to be sequestered within the myocyte fibers (Figs. 7 and 8).

4. Discussion

To our knowledge, this is the first report on the analysis of mechanical function ex vivo of hearts isolated from aortically constricted mice. Until now, such studies have been carried out, usually on anesthetized mice, using echocardiography or intraventricular pressure-volume catheterization in situ [2,21,22]. A notable finding here is that aortic banding in the mouse produces distinct time-dependent alterations in both diastolic and systolic indices of LV function assessed ex vivo that are not entirely consistent with results of analogous echocardiographic studies. On the one hand, the development of diastolic dysfunction, quantified by increases in LVEDP and LVEDV (Table 2, Fig. 2), was comparable to results obtained echocardiographically [2,9,21]. This was associated with similar time-dependent increases in LW and reductions in BW (Table 1), confirming a progressive development of HF in this model [9,23]. On the other hand, the significant reductions in direct and indirect indexes of systolic function, including LVESP, SV, ejection fraction,

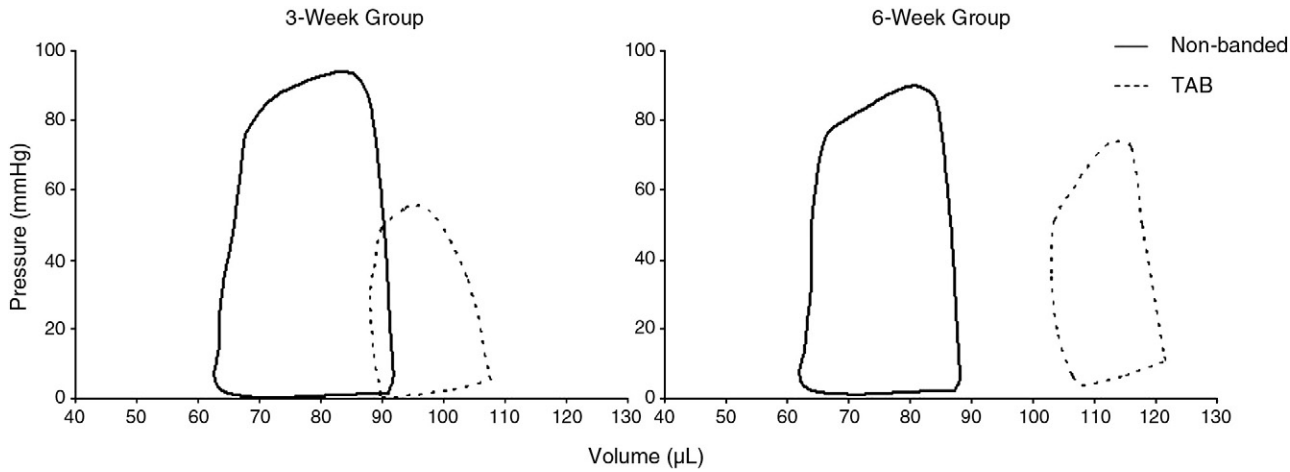

Fig. 3. Representative pressure–volume loops generated by perfused working hearts from TAB and age-matched non-banded mice at 3 and 6 weeks post-banding.

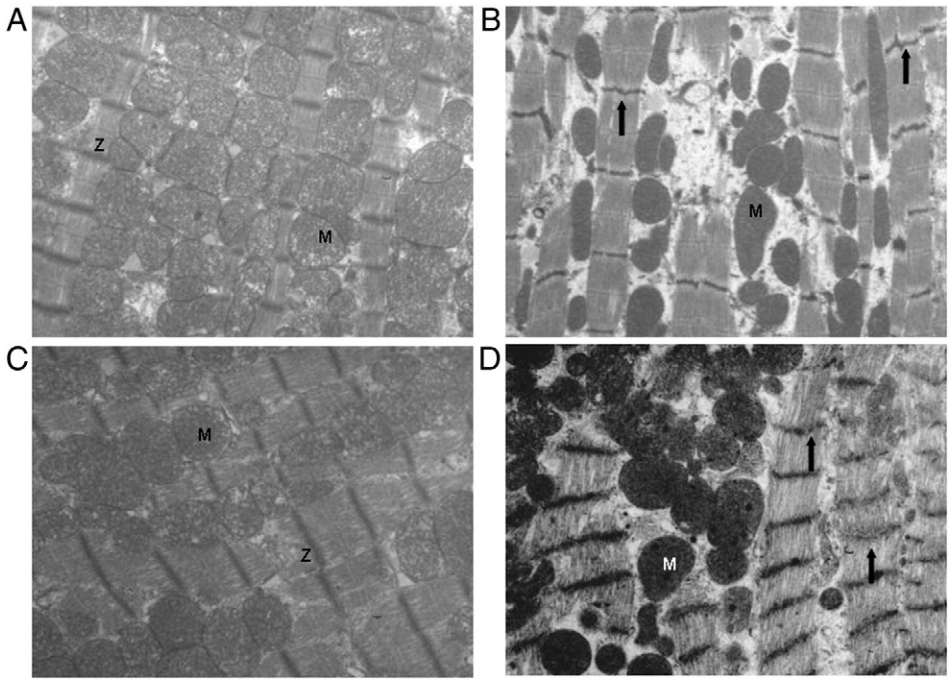

Fig. 5. Myocardial Z-band derangement during the development of cardiac hypertrophy. Micrographs of the LV apex of non-banded (A, C) and TAB (B, D) mice presenting with extensive Z-band damage at 3 weeks with regression at 6 weeks post banding. M, mitochondria; Z, normal Z-band; ↑, damaged Z-band.

CO, and +dP/dt, evident at 3 and 6 weeks post-banding (Table 2, Figs. 1 and 3), were somewhat different from the pattern displayed by TAB mice in vivo. Measurements taken by echocardiography or catheterization show that LV peak pressure and + or −dP/dt in vivo are either unchanged or elevated as early as 2 weeks, and as much as 9 weeks, following aortic banding [3,21].

The discrepancy between our results and those obtained in vivo, regarding alterations in systolic function produced by TAB, is not surprising. Function of all hearts was assessed here at identical pressure load (resistance to aortic outflow) and volume load (left atrial filling pressure). Both of these loads, however, would be expected to be higher in the banded than in the non-banded mouse in vivo, and thus peak systolic LV pressure generation and related variables would be elevated accordingly, unless the hearts are in late-stage, severe congestive heart failure [23]. Constant pressure loading may also explain, at least in part, the lower SV and CO values of the somewhat larger hearts from the control group at six weeks (Table 2). Our results indicate that chronic aortic banding depresses intrinsic contractility of the hypertrophic heart within 3 weeks, which may be masked in vivo by cardiac autoregulatory responses to variable hemodynamic conditions.

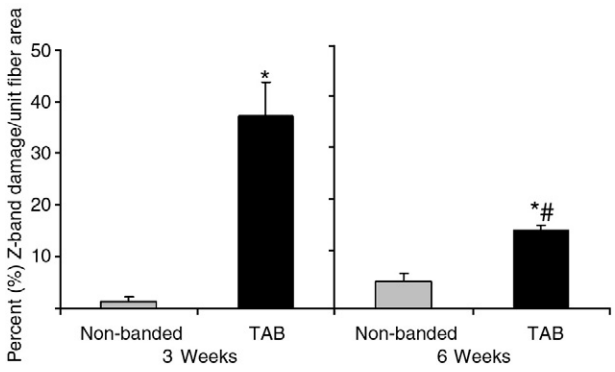

Fig. 6. Percent of DZF per unit fiber area in the LV apex of TAB and non-banded mice at 3 and 6 weeks post banding. n=5 per group. Values are means± S.E.M. *Significantly different from age-matched non-banded group, P<.05; #significantly different from 3 week banded group, P<.05.

A second new observation in this study was the reduction in the rate of glycolytic flux after aortic banding in the mouse, which by 6 weeks had declined to levels that were approximately 55 % that of the control hearts (Fig. 4). Generally, glycolytic flux is assumed to increase in LVH of various etiologies [7,24-26]. The response is presumably related largely to increases in glucose uptake, and expressions of sarcolemmal GLUT1 or GLUT4 transporters and possibly of glycolytic enzymes as well [8,27,28]. However, if the focus is restricted specifically to LVH secondary to high external pressure loads (as opposed to coronary ischemia or myocardial infarction, transgenic models of hypertrophic cardiomyopathy, and so forth), the pattern is not as straightforward. For example, aortic banding in the rat increases glycolysis [7], glucose uptake, and the expression of GLUT1, but has no effect on the expression of GLUT4 [24,29]. In contrast, aortic banding in the rabbit decreases myocardial glucose uptake with no marked alterations in the expression of either GLUT1 or GLUT4 [30]. Interestingly, aortic banding in the mouse produces an early increase in

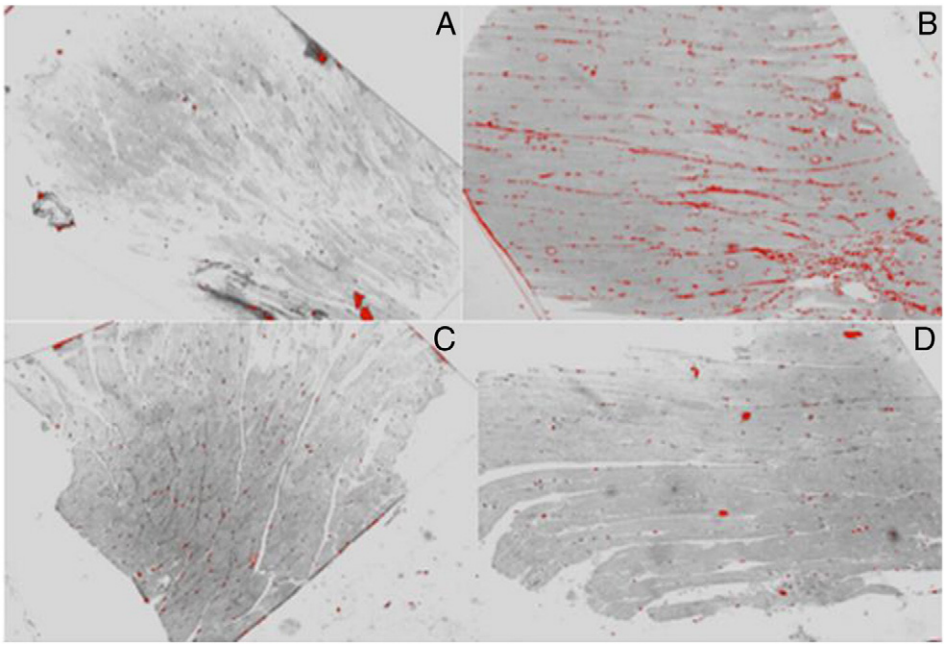

Fig. 7. Collagen staining of the LV apex of non-banded (A, C) and TAB (B, D) mice presenting with extensive collagen deposition at 3 weeks (B) with regression at 6 weeks (D) post-banding.

GLUT1 expression with no corresponding increase in glucose uptake [9,31]. The last is consistent with our findings that glycolysis does not markedly change until failure develops later on (Figs. 2 and 4). Parallel alterations in glucose transporter expression, which might account for the decrease in glycolysis over time in this mouse model, remain to be investigated. Increased utilization of glucose in LVH has been characterized as an adaptive metabolic remodeling response to chronically high pressure loads, in part because if its presumably favorable effects on intracellular ratios of high energy phosphates [8]. By that reasoning, declines in glycolytic rates, as observed here, would be maladaptive [6]. In support of this view, ventricular function is markedly depressed in hypertrophic mouse hearts when GLUT4 is knocked out [32,33], but partially preserved if GLUT1 transporters are overexpressed [9].

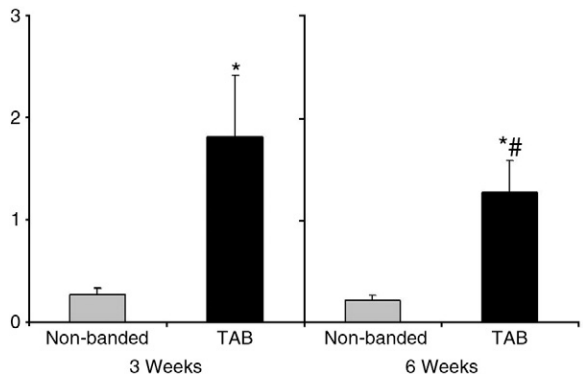

Fig. 8. Quantification of collagen deposition from TAB and age-matched non-banded mice at 3 and 6 weeks post banding. Y axis values are percentages of total area in the field occupied by collagen staining. Values are means± S.E.M. *Significantly different from age-matched non-banded group, $P<.05$; #significantly different from 3-week control group, $P<.05$.

The decline in mechanical function in TAB hearts was also associated with specific structural abnormalities in the left ventricle. As reported previously for rat models of pressure overload hypertrophy [34-36], we observed here a profound disruption of myocyte Z-band integrity in the hypertrophic mouse ventricle that was not associated with discernable evidence of abnormal mitochondrial structure (Figs. 5 and 6). Similarly, marked collagen deposition was evident here at 3 and 6 weeks following aortic constriction with an apparent downward trend observed from three to 6 weeks in TAB mice (Figs. 7 and 8). These findings are consistent with previous reports of temporal changes in the extent of ventricular collagen deposition in aortically banded mice [2] and ferrets [20]. A loss of interstitial collagen may contribute importantly to the transition from compensated hypertrophy to HF and may involve altered expressions and activities of tissue inhibitors of metalloproteinase Type 3 [37] and matrix metalloproteinase Type 9 [20].

In summary, the results reported here indicate that the isolated working mouse heart preparation is a useful method to assess cardiac function and metabolism during the development of hypertrophic HF. Analysis of function ex vivo reveals that aortic banding rapidly depresses intrinsic LV contractility in this model, an effect that is not consistently observed in vivo. A novel finding is that glycolytic flux declines as diastolic dysfunction and failure progress, suggesting that metabolic remodeling involving glucose utilization is maladaptive in this model of mouse heart hypertrophy.

5. Summary

This work describes cardiac ultrastructural, functional, and metabolic derangements associated with the development of left ventricular hypertophy and heart failure in the aortically banded mouse. A progressive decline in glycolytic flux suggests that altered glucose metabolism is maladaptive in this failure model.

Acknowledgments

The authors wish to acknowledge the excellent technical assistance provided by Dr. Alia Morgham of the Department of Kinesiology at the University of Rhode Island. This work was supported in part by NSF Grant BES-0448050, RI-INBRE Grant #P20RR016457 from the National Center for Research Resources, a component of the NIH and the American Foundation for Pharmaceutical Education Pre-Doctoral Fellowship.

References

[1] Cantor EJ, Babick AP, Vasanji Z, Dhalla NS, Netticadan T. A comparative serial echocardiographic analysis of cardiac structure and function in rats subjected to pressure or volume overload. J Mol Cell Cardiol 2005;38(5):777–86.
[2] Foronjy RF, Sun J, Lemaitre V, D'Armiento JM. Transgenic expression of matrix metalloproteinase-1 inhibits myocardial fibrosis and prevents the transition to heart failure in a pressure overload mouse model. Hypertens Res 2008;31(4):725–35.
[3] Gelpi RJ, Gao S, Zhai P, et al. Genetic inhibition of calcineurin induces diastolic dysfunction in mice with chronic pressure overload. Am J Physiol Heart Circ Physiol 2009;297(5):H1814–9.
[4] Chatterjee K, Massie B. Systolic and diastolic heart failure: differences and similarities. J Card Fail 2007;13(7):569–76.
[5] Vinet L, Rouet-Benzineb P, Marniquet X, et al. Chronic doxycycline exposure accelerates left ventricular hypertrophy and progression to heart failure in mice after thoracic aorta constriction. Am J Physiol Heart Circ Physiol 2008;295(1):H352–60.
[6] Sambandam N, Lopaschuk GD, Brownsey RW, Allard MF. Energy metabolism in the hypertrophied heart. Heart Fail Rev 2002;7(2): 161–73.
[7] Schonekess BO, Allard MF, Lopaschuk GD. Recovery of glycolysis and oxidative metabolism during postischemic reperfusion of hypertrophied rat hearts. Am J Physiol 1996;271(2 Pt 2):H798–805.
[8] Ingwall JS. Energy metabolism in heart failure and remodelling. Cardiovasc Res 2009;81(3):412–9.
[9] Liao Y, Ishikura F, Beppu S, et al. Echocardiographic assessment of LV hypertrophy and function in aortic-banded mice: necropsy validation. Am J Physiol Heart Circ Physiol 2002;282(5):H1703–8.
[10] Pacher P, Nagayama T, Mukhopadhyay P, Batkai S, Kass DA. Measurement of cardiac function using pressure-volume conductance catheter technique in mice and rats. Nat Protoc 2008;3(9):1422–34.
[11] How OJ, Aasum E, Severson DL, Chan WY, Essop MF, Larsen TS. Increased myocardial oxygen consumption reduces cardiac efficiency in diabetic mice. Diabetes 2006;55(2):466–73.
[12] van Oort RJ, Respress JL, Li N, et al. Accelerated development of pressure overload-induced cardiac hypertrophy and dysfunction in an RyR2-R176Q knockin mouse model. Hypertension 2010;55(4): 932–8.
[13] Gupta S, Sen S. Animal models for heart failure. Methods Mol Med 2006;129:97–114.
[14] Aasum E, Belke DD, Severson DL, et al. Cardiac function and metabolism in Type 2 diabetic mice after treatment with BM 17.0744, a novel PPAR-alpha activator. Am J Physiol Heart Circ Physiol 2002; 283(3):H949–57.
[15] Morgan HE, Neely JR, Wood RE, Liebecq C, Liebermeister H, Park CR. Factors affecting glucose transport in heart muscle and erythrocytes. Fed Proc 1965;24(5):1040–5.
[16] Rodgers RL. The Working Rat Heart Preparation. In: McNeil JH, editor. Measurement of Cardiac Function. Florida: CRC Press, Inc, 1997. p. 11–40.
[17] Rodgers RL, Christe ME, Tremblay GC, Babson JR, Daniels T. Insulin-like effects of a physiologic concentration of carnitine on cardiac metabolism. Mol Cell Biochem 2001;226(1-2):97–105.
[18] Harney JA, Rodgers RL. Insulin-like stimulation of cardiac fuel metabolism by physiological levels of glucagon: involvement of PI3K but not cAMP. Am J Physiol Endocrinol Metab 2008;295(1): E155–61.
[19] Weibel ER. Stereological principles for morphometry in electron microscopic cytology. Int Rev Cytol 1969;26:235–302.
[20] Graham HK, Trafford AW. Spatial disruption and enhanced degradation of collagen with the transition from compensated ventricular hypertrophy to symptomatic congestive heart failure. Am J Physiol Heart Circ Physiol 2007;292(3):H1364–72.
[21] Hu P, Zhang D, Swenson L, Chakrabarti G, Abel ED, Litwin SE. Minimally invasive aortic banding in mice: effects of altered cardiomyocyte insulin signaling during pressure overload. Am J Physiol Heart Circ Physiol 2003;285(3):H1261–9.
[22] Oudit GY, Kassiri Z, Zhou J, et al. Loss of PTEN attenuates the development of pathological hypertrophy and heart failure in response to biomechanical stress. Cardiovasc Res 2008;78(3):505–14.
[23] Fukuta H, Little WC. Diagnosis of diastolic heart failure. Curr Cardiol Rep 2007;9(3):224–8.
[24] Degens H, de Brouwer KF, Gilde AJ, et al. Cardiac fatty acid metabolism is preserved in the compensated hypertrophic rat heart. Basic Res Cardiol 2006;101(1):17–26.
[25] Lydell CP, Chan A, Wambolt RB, et al. Pyruvate dehydrogenase and the regulation of glucose oxidation in hypertrophied rat hearts. Cardiovasc Res 2002;53(4):841–51.
[26] Stanley WC, Recchia FA, Lopaschuk GD. Myocardial substrate metabolism in the normal and failing heart. Physiol Rev 2005;85(3): 1093–129.
[27] Depre C, Rider MH, Hue L. Mechanisms of control of heart glycolysis. Eur J Biochem 1998;258(2):277–90.
[28] Krishnan J, Suter M, Windak R, et al. Activation of a HIF1alpha-PPARgamma axis underlies the integration of glycolytic and lipid anabolic pathways in pathologic cardiac hypertrophy. Cell Metab 2009;9(6):512–24.
[29] Tian R, Musi N, D'Agostino J, Hirshman MF, Goodyear LJ. Increased adenosine monophosphate-activated protein kinase activity in rat hearts with pressure-overload hypertrophy. Circulation 2001;104(14): 1664–9.
[30] Takeuchi K, McGowan FX, Glynn P, et al. Glucose transporter upregulation improves ischemic tolerance in hypertrophied failing heart. Circulation 1998;98(19 Suppl):II234–9.
[31] Morissette MR, Howes AL, Zhang T, Heller BJ. Upregulation of GLUT1 expression is necessary for hypertrophy and survival of neonatal rat cardiomyocytes. J Mol Cell Cardiol 2003;35(10): 1217–27.
[32] Domenighetti AA, Danes VR, Curl CL, Favaloro JM, Proietto J, Delbridge LM. Targeted GLUT-4 deficiency in the heart induces cardiomyocyte hypertrophy and impaired contractility linked with Ca (2+) and proton flux dysregulation. J Mol Cell Cardiol 2010;48(4): 663–72.
[33] Huggins CE, Domenighetti AA, Ritchie ME, et al. Functional and metabolic remodelling in GLUT4-deficient hearts confers hyper-responsiveness to substrate intervention. J Mol Cell Cardiol 2008;44 (2):270–80.

[34] Anversa P, Vitali-Mazza L, Visioli O, Marchetti G. Experimental cardiac hypertrophy: a quantitative ultrastructural study in the compensatory stage. J Mol Cell Cardiol 1971;3(3):213–27.
[35] Matlib MA, Rembert JC, Millard RW, et al. Mitochondrial function in canine experimental cardiac hypertrophy. J Mol Cell Cardiol 1983;15 (4):221–32.
[36] Wendt-Gallitelli MF, Ebrecht G, Jacob R. Morphological alterations and their functional interpretation in the hypertrophied myocardium of Goldblatt hypertensive rats. J Mol Cell Cardiol 1979;11(3):275–87.
[37] Fedak PW, Altamentova SM, Weisel RD, et al. Matrix remodeling in experimental and human heart failure: a possible regulatory role for TIMP-3. Am J Physiol Heart Circ Physiol 2003;284(2):H626–34.